Available online at Wisvora

Journal of Global Governance and Sustainability

Journal homepage: https://wisvora.com/index.php/jggs/index

Automated and sustainable coating assessment for H-shaped steel using DNN

Diana Wahyu Hayati[1], Jieh-Haur Chen[2*], Mu-Chun Su[3], Wei-Jen Lin[4], and Ting-Kwei Wang[5]

[1] Post-doctoral Research Fellow, Department of Civil Engineering, National Central University, Jhongli, Taoyuan 320317, Taiwan.
[2]Distinguished Professor, Department of Civil Engineering; Director, Research Center of Smart Construction; and Associate Dean, College of Engineering, National Central University, Zhongli, Taoyuan 320317, Taiwan.
[3] Distinguished Professor, Department of Computer Science and Information Engineering, National Central University, Zhongli, Taoyuan 320317, Taiwan.
[4] PhD Candidate, Department of Computer Science and Information Engineering, National Central University, Zhongli, Taoyuan 320317, Taiwan.
[5]Associate Professor, Department of Civil Engineering, National Kaohsiung University of Science and Technology, Kaohsiung 81164, Taiwan.

ABSTRACT

This study presents the development of a fully automated recognition system leveraging Deep Neural Networks (DNN) to identify and evaluate coating patterns and structural attributes of H-shaped steel components. The system is designed not only to improve the efficiency and accuracy of inspection processes but also to contribute to sustainable construction practices by enabling early defect detection, reducing material waste, and optimizing lifecycle maintenance. The computational pipeline consists of eight key stages: (1) data input, (2) detection area computation, (3) categorization of residual regions, (4) calculation of potential parallel distances, (5) optimal pattern recognition, (6) model-object comparison, (7) output generation for Matplotlib visualization, and (8) 3D plot construction from output coordinates. This pipeline allows for precise, non-destructive evaluation and facilitates real-time integration into automated fabrication or quality control workflows. The system was trained and validated using a robust dataset comprising 115 standard-type and 99 special-type H-shaped steel samples, representing a broad spectrum of commercially used profiles. The proposed model achieved 100% accuracy in identifying critical geometric features such as width, base plate thickness, and wing plate thickness. The overall recognition accuracy exceeded 99.12%, with an average real-world application accuracy of 99.73%, indicating excellent performance and reliability for industrial deployment. By automating the recognition process and enhancing the reliability of coating and structural assessments, this research supports the development of smart, resource-efficient infrastructure, aligning with key goals in sustainable manufacturing and resilient civil engineering.

KEYWORDS

H-shaped steel component, Deep Neural Networks (DNN), pattern recognition, coating, automation, sustainable assessment

* *Corresponding author: Jieh-Haur Chen* (e-mail: jhchen@ncu.edu.tw)

Received November 3, 2025; Accepted December 15, 2025
Available online December 26, 2025

1. INTRODUCTION

Steel plays a pivotal role within the construction sector, finding application in both reinforced concrete buildings and steel-framed constructions. The suitability of steel usage is predicated on its structural characteristics. While steel structures offer numerous advantages such as impressive load-bearing capacity, reduced weight relative to concrete counterparts, and favorable plasticity and toughness, they are also prone to drawbacks such as inadequate fire resistance and vulnerability to corrosion due to inherent material properties. These limitations can undermine the stability and longevity of H-shaped steel elements, leading to decreased safety and overall structural lifespan. To address these challenges, a common strategy involves the application of a protective coating to the steel surface, bolstering its resistance to fire and corrosion. This protective layer acts as a barrier, preventing the formation of rust [1]. The two primary methods widely employed for applying coatings to steel surfaces are metal coating [2] and organic coating [3].

H-shaped steel components find frequent use in steel-framed buildings as beam and column supports, in steel-structured bridges, as well as in geotechnical engineering and building foundations. Preserving the physical properties of this material is imperative to prevent damage and unforeseen incidents. Hence, this study focuses on automated pattern recognition for H-shaped steel within the context of the coating process. Presently, manual techniques dominate the treatment of H-shaped steel surfaces. However, technological progress offers more efficient and convenient avenues. Manual methods heavily rely on human labor, exposing workers to potential hazards during coating and processing procedures. Furthermore, the manual coating process lacks consistency (e.g., fixed spraying angles and paths), posing challenges in achieving uniform coating thickness. Automating this process holds the potential to enhance coating quality, reduce operator exposure to hazardous materials, and contribute to the advancement of steel structural engineering. Consequently, further research is warranted to develop automated coating techniques for H-section steel and to propel advancements in the field of steel structural engineering.

Two predominant techniques are commonly utilized for automated spray procedures. The initial method involves employing a robotic arm to perform the task, while the second approach uses a fixed apparatus to spray objects as they traverse a conveyor belt. Between these two strategies, the former holds a clear advantage over the latter due to its heightened adaptability throughout the coating process. Nonetheless, integrating robotic arms for task execution requires incorporating a pattern recognition system for target identification and devising paths for task completion [4]. Pattern recognition functions as the "vision" of the robotic arm, enabling it to discern and gather surface-related data about the target. This encompasses various aspects such as target position, shape, contour, size, cross-sectional area, and other spatial particulars [5, 6]. Conversely, path planning acts as the "brain" of the robotic arm, charting a trajectory for the arm to accomplish the required tasks on the identified target. Undoubtedly, the process of planning the path involves numerous assumptions that require careful consideration. Therefore, the fusion of pattern recognition and path planning serves as the foundation for creating an automated process. In its simplest iteration, after identifying the target, the optimal path for completing the task is determined. Subsequently, the robotic arm executes the process on the target in accordance with the designated path.

The objective of this study is to establish a three-dimensional automated identification system focused on extracting surface-related information. This extracted data serves as a fundamental input for subsequent path planning within an automated coating system tailor-made for H-section steel.

2. APPLICATIONS FOR PATTERN RECOGNITION IN CONSTRUCTION

Integrating pattern recognition into an automated coating system designed for H-shaped steel components holds significant importance for their detection and analysis. By processing captured images and utilizing existing models, computer calculations generate crucial geometric and positional coordinate data. These outputs play a vital role in the subsequent path planning required to effectively apply surface coatings to the steel objects. Pattern recognition is intricately tied to the extraction of information from images or objects [5, 7], encompassing attributes like shape, outline, texture, size, and color

[5, 6]. In the context of this study, the implementation of pattern recognition involves the initial characterization of H-shaped steel objects based on relevant images or models.

Subsequently, these features are utilized for calculations and analyses to construct a model of the H-shaped steel. Previous research has explored the utilization of pattern recognition in various domains, albeit to a limited extent. For example, Armingol et al. (2003) employed pattern recognition to evaluate metal quality through visual images [8]. Balsamo et al. (2014) utilized pattern recognition to discern structural conditions [9], while Babic et al. (2018) applied it to estimate the hardness of a laser quenching machine [10]. Michaelsen and Meidow (2014) employed pattern recognition to identify structural landmarks [11], and Wallhauser et al. (2011) used it to detect scale formation on stainless steel. Other studies have adapted pattern recognition methodologies for diverse aims and functions[12-18]. Prior investigations have demonstrated that pattern recognition can effectively identify errors, defects, and damage patterns in products and materials, thereby contributing to control and implementation efforts.

Pattern recognition can be classified into two primary categories: conventional pattern recognition and artificial intelligence pattern recognition. Conventional pattern recognition includes global or statistical pattern recognition and structural pattern recognition methodologies [5, 6, 19]. In the case of global or statistical pattern recognition, space vector information is obtained through statistical calculations based on identified feature data[5, 20]. Although this approach provides higher accuracy, it requires greater information storage and is less adept at handling irregular characteristic data [5]. On the other hand, structural pattern recognition divides the object of recognition into distinct components based on different structural forms or characteristics. Mathematical calculations are then performed on the boundary conditions of each component to generate representative space vector information[5, 20]. While this method allows for the processing of obscured object parts, it involves more complex computational procedures [5].

Artificial intelligence pattern recognition, conversely, employs computational techniques based on machine learning [21]. The method employed in this study, known as the Deep Neural Network (DNN), falls within the realm of artificial intelligence pattern recognition and comprises three layers of neural networks: input, hidden, and output layers[21-23]. In this method, the weights of a training dataset are fed into the first layer, then processed through the hidden layer to create the desired model. Neural networks necessitate substantial training using extensive datasets, making them particularly effective for complex problems rich in information. Nonetheless, the success of this approach relies heavily on the computational power of the computer and the amount of training data available[24].

Prior investigations have delved into the deployment of pattern recognition across various domains within the realm of steel and steel structures. These studies encompass a diverse spectrum of applications. For instance, they explore the utilization of fence sensors and conveyor belts for structural pattern recognition [25], employ structural pattern recognition techniques to identify bridge steel [26], diagnose damage in steel structures through signal-based pattern recognition [27], estimate stress in steel structural elements using subset mode pattern recognition for structural health monitoring [28], and automatically detect corrosion in bridge steel bars embedded within concrete using ground-penetrating radar [29]. Moreover, the combination of pattern recognition, image acquisition, and analysis has been integrated with optimized machine learning algorithms to characterize steel bars [30]. The application of structural pattern recognition prominently surfaces in the identification of steel components, primarily due to their relatively straightforward attributes encompassing shape, contour, texture, size, and color.

Segmenting the object into distinct parts streamlines the process of identification, contributing to enhanced convenience and accuracy. Beyond its application in steel-related contexts, pattern recognition technology has garnered widespread usage across diverse domains within the field of civil engineering. For instance, Zeghal and Abdel-Ghaffar (1992) employed seismic records and identification systems to analyze earthquake-induced behavior in earth-rock dams [31]. Abdel Razig and Chang (2000) utilized neural networks and image processing to establish a computer-executed system for defect recognition and measurement [32]. Zhang, Cheng, and Wang (2018) leveraged principal component analysis and multi-type support vector machines to classify and identify observation data in hot-mix asphalt production [33]. Brilakis, German, and Zhu (2011) introduced a framework for the automated identification of infrastructure-related elements using visual pattern recognition based on remotely sensed visual feature data [34]. The aforementioned examples underscore the versatility of pattern recognition, which finds practical applications in civil engineering for analysis, detection, management, and modelling endeavours.

3. DESIGN OF DNN-ENHANCED DETECTION MODEL

In order to develop a pattern recognition methodology for coating H-shaped steel, it's crucial to construct a surface profile model of the H-shaped steel object that can be utilized for planning the coating path. The following assumptions have been taken into account:

(1) The primary emphasis of this investigation is directed towards the analysis of H-shaped steel beams.
(2) The H-shaped steel beam being investigated.
(3) The selection of the Stereolithography (STL) model file format is based on its widespread utilization in coating factories. This format represents models through the use of triangles.
(4) A substantial sample set exceeding 70 pieces has been gathered from a coating factory.
(5) The dimensions of the H-shaped steel samples considered in this study encompass a range from 100 x 50 x 1,000 mm to 900 x 300 x 10,000 mm (height x width x length).

The unique attributes of H-shaped steel items encompass symmetry between their left and right facets, symmetry between their upper and lower facets, and symmetry between their starting and concluding segments, as illustrated in Figure 1.

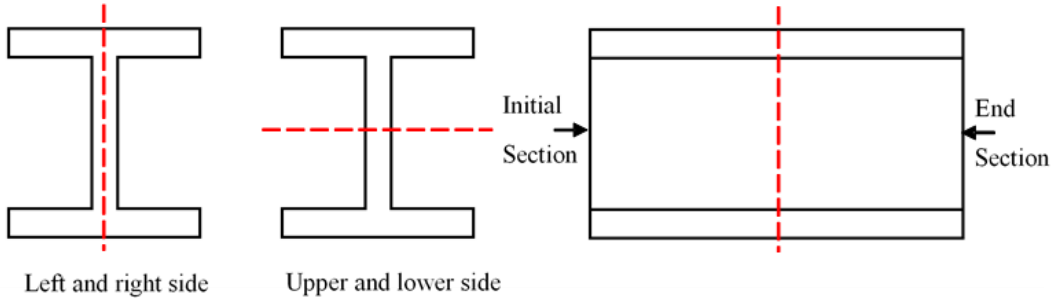

Figure 1 Symmetry of the H-shaped steel beam

4. DNN-ENHANCED DETECTION MODEL

By utilizing the STL model format, the H-shaped steel models can be deconstructed into groupings of triangular surfaces. This methodology enables to extract size parameters and establish a surface profile model. Through the application of the STL model, calculations are performed to analyze the plane equations and normal vectors for each triangle within the model. These plane equations are iteratively processed, preserving the x, y, and z axes within the normal vector and spatial coordinates aligned with a specific axis. The categorization of each plane is contingent on the coordinate axis, facilitating the determination of viable combinations of length, width, and height for the H-shaped steel model. Following this, the DNN is employed to determine the most appropriate set of size parameters. This determination is achieved by comparing the STL model to the actual H-shaped steel object, ensuring optimal consistency and recognition accuracy.

The selected configuration for image and video pattern recognition involves a [30, 30, 30, 30, 30] DNN classifier, combined with a 7-click sliding window approach. This methodology aims to diminish noise, amplify recognition precision, enhance operational efficiency, and elevate accuracy [35]. Upon determining the size parameters through the STL model file, Python's Matplotlib software is employed to generate 3D spatial coordinates, ultimately culminating in the visualization of the 3D contours of the H-shaped steel model. To align with industry practicality, a recognition rate of 99% is specified, while maintaining an error tolerance of 1%. The comprehensive automated process for fabricating the H-shaped steel model for coating is visually illustrated in Figure 2, encompassing two principal constituents: 1) acquiring H-shaped steel size parameters; and 2) constructing the H-shaped steel coating model.

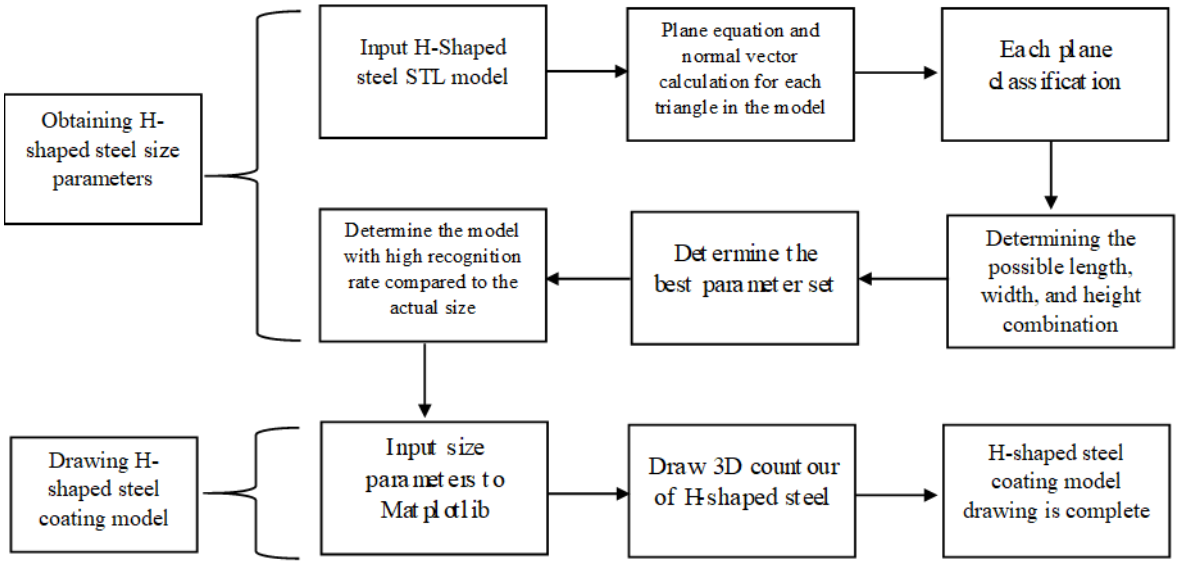

Figure 2 H-shaped steel pattern recognition method

5. MODEL VERSIFICATION AND DISCUSSION

To verify the precision of the model in faithfully representing actual H-shaped steel objects, the ensuing steps are undertaken. In the event of an inconsistency within the size parameter, an analysis of the STL model is performed to identify any anomalies that could be contributing to the discrepancy. Disproportionate data or excessive information contained within a single model file might trigger such deviations (e.g., having two instances of length recorded in the model). Should the model itself be deemed reliable, adjustments are applied to the size acquisition algorithm, followed by a reassessment of the parameter. If the model exhibits an abnormal condition that doesn't affect the size parameters, the drawing process proceeds accordingly. However, if the irregularities within the STL model influence the outcomes of the size parameters, corrective measures are applied to rectify the problematic execution logic. Furthermore, a meticulous documentation of the contour drawing process is maintained to facilitate discussions on the results and troubleshooting. The findings from the evaluation of size parameters are presented in the Appendix. A juxtaposition with the actual dimensions of the authentic H-shaped steel object reveals a complete alignment, where every calculated size parameter accurately corresponds to the real dimensions. This achievement is attributed to the STL model file solely comprising standard H-shaped steel objects, excluding specialized types. Consequently, a recognition rate of 100% is realized across all size parameters.

These findings stand as substantiation that this approach adeptly acquires size parameters for standard H-shaped steel objects. A visual representation of the standard H-shaped steel is depicted in Figure 3. The results of a comparative analysis of size parameters for specialized H-shaped steel types are detailed in both Table 1 and Table 2. These tables showcase recognition rates that exceed 99%, affirming the precise determination of parameters. From Table 2, it becomes evident that dimensions such as width, web thickness, and flange thickness demonstrate a perfect 100% accuracy in identification. While the recognition rate for length, height, and end connecting plate might not attain the full 100%, it consistently surpasses 99% for the majority of cases (with the exception of special type 7, which deviates in length from the other six types). Recognition rates for special cases range from 99.19% to 99.81%, whereas for special type 7, the recognition rate for length and height is recorded at 27.82% and 53.00% respectively. The overall identification rate for size parameters stands at 99.73%. A visual depiction of specialized H-shaped steel types is furnished in Figure 4.

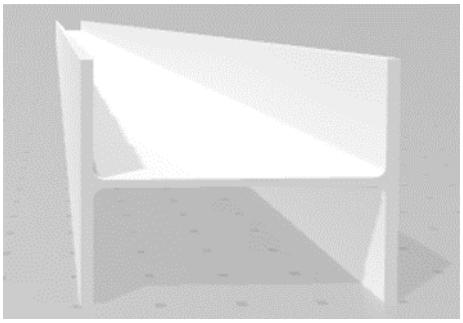

Figure 3 Standard type H-shaped steel beam

Table 1 Size parameter identification of special types of H-shaped steel

Model list	Total model	Correct length	Correct height	Correct width	Correct web thickness	Correct flange plate thickness
Special type 1 (screw nut)	41	41	41	41	41	41
Special type 2 (screw nut and end connecting plate)	18	18	18	18	18	18
Special type 3 (screw nut, hook and end connecting plate)	26	26	26	26	26	26
Special type 4 (screws, nuts, end connecting plate and middle L-shaped connecting plate)	4	4	4	4	4	4
Special type 5 (screws, nuts and partitions)	5	5	5	5	5	5
Special type 6 (screws, nuts, partitions, end connecting plate and middle connecting plate)	4	4	4	4	4	4
Special type 7 (Other)	1	0	0	1	1	1
Total	99	98	98	99	99	99

Table 2 Size parameter recognition rate for special types of H-shaped steel

Model list	Length: correct recognition rate	Height: correct recognition rate	Width: correct recognition rate	Web thickness: correct recognition rate	Flange thickness: correct recognition rate
Special type 1 (screw nut)	100.00%	100.00%	100.00%	100.00%	100.00%
Special type 2 (screw nut and end connecting plate)	99.69%	100.00%	100.00%	100.00%	100.00%
Special type 3 (screw nut, hook and end connecting plate)	99.72%	100.00%	100.00%	100.00%	100.00%
Special type 4 (screws, nuts, end connecting plate and middle L-shaped connecting plate)	99.79%	100.00%	100.00%	100.00%	100.00%

Model list	Length: correct recognition rate	Height: correct recognition rate	Width: correct recognition rate	Web thickness: correct recognition rate	Flange thickness: correct recognition rate
Special type 5 (screws, nuts and partitions)	100.00%	100.00%	100.00%	100.00%	100.00%
Special type 6 (screws, nuts, partitions, end connecting plate and middle connecting plate)	99.58%	100.00%	100.00%	100.00%	100.00%
Special type 7 (Other)	27.82%	53.00%	100.00%	100.00%	100.00%
Overall correct recognition rate	99.12%	99.53%	100.00%	100.00%	100.00%

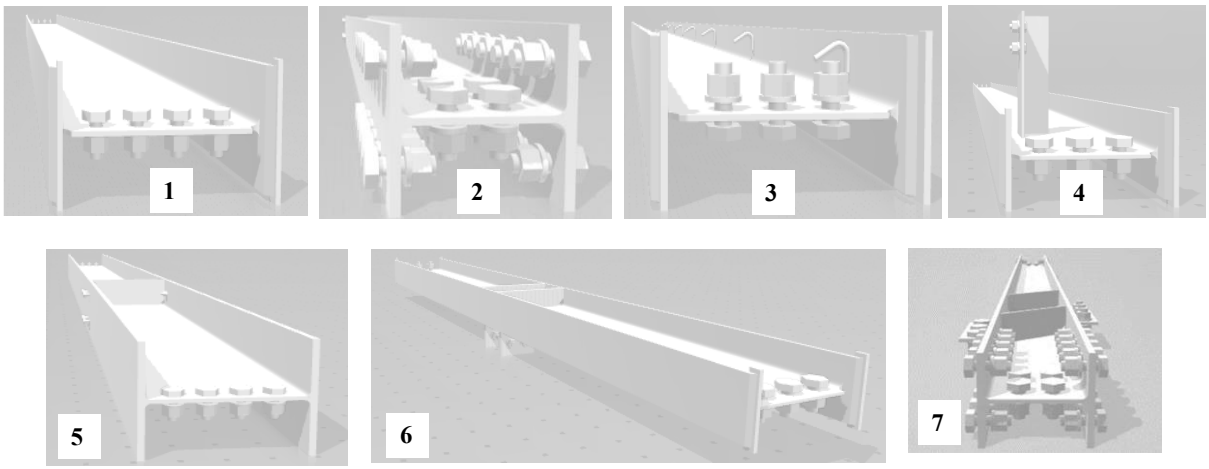

Figure 4 Special types of H-shaped steel

To validate the accuracy and feasibility of the outcomes, a verification procedure is executed. In the course of this validation process, a comparison is drawn between the derived size parameters and the actual dimensions to uncover any disparities. The encountered challenges predominantly emanate from the STL model of the H-shaped steel. The initial challenge arises due to slight deviations between the length and dimension parameters of the H-shaped steel object and its authentic specifications. This variance mainly emerges from the inclusion of connecting plates at the ends of certain STL models. Consequently, the measured length surpasses the length of the connecting plate. Furthermore, the length in the genuine specifications is solely calculated for standard H-section steel types, contributing to minor inconsistencies in length. While this matter has been acknowledged, it hasn't been rectified through program modification. This decision is influenced by the fact that the program doesn't generate errors while capturing the cross-sectional dimensions of the H-shaped steel object, and the accurate model can still be established. The second predicament pertains to the challenge of precisely retrieving the length and height dimension parameters for special type 7 H-shaped steel. This issue arises primarily due to the presence of both a partition and a connecting plate within the H-shaped steel structure, which confounds the algorithm's ability to accurately distinguish between these components.

6. CONCLUSION

To verify the precision of the model in faithfully representing actual H-shaped steel objects, the ensuing steps are undertaken. In the event of an inconsistency within the size parameter, an analysis of the STL model is performed to identify any anomalies that could be contributing to the discrepancy. Disproportionate data or excessive information contained within a single model file might trigger such deviations (e.g., having two instances of length recorded in the model). Should the model itself be deemed reliable, adjustments are applied to the size acquisition algorithm, followed by a reassessment of the parameter. If the model exhibits an abnormal condition that doesn't affect the size parameters, the drawing process proceeds

accordingly. However, if the irregularities within the STL model influence the outcomes of the size parameters, corrective measures are applied to rectify the problematic execution logic. Furthermore, a meticulous documentation of the contour drawing process is maintained to facilitate discussions on the results and troubleshooting. The findings from the evaluation of size parameters are presented in the Appendix. A juxtaposition with the actual dimensions of the authentic H-shaped steel object reveals a complete alignment, where every calculated size parameter accurately corresponds to the real dimensions. This achievement is attributed to the STL model file solely comprising standard H-shaped steel objects, excluding specialized types. Consequently, a recognition rate of 100% is realized across all size parameters.

These findings stand as substantiation that this approach adeptly acquires size parameters for standard H-shaped steel objects. A visual representation of the standard H-shaped steel is depicted in Figure 3. The results of a comparative analysis of size parameters for specialized H-shaped steel types are detailed in both Table 1 and Table 2. These tables showcase recognition rates that exceed 99%, affirming the precise determination of parameters. From Table 2, it becomes evident that dimensions such as width, web thickness, and flange thickness demonstrate a perfect 100% accuracy in identification. While the recognition rate for length, height, and end connecting plate might not attain the full 100%, it consistently surpasses 99% for the majority of cases (with the exception of special type 7, which deviates in length from the other six types). Recognition rates for special cases range from 99.19% to 99.81%, whereas for special type 7, the recognition rate for length and height is recorded at 27.82% and 53.00% respectively. The overall identification rate for size parameters stands at 99.73%. A visual depiction of specialized H-shaped steel types is furnished in Figure 4.

To validate the accuracy and feasibility of the outcomes, a verification procedure is executed. In the course of this validation process, a comparison is drawn between the derived size parameters and the actual dimensions to uncover any disparities. The encountered challenges predominantly emanate from the STL model of the H-shaped steel. The initial challenge arises due to slight deviations between the length and dimension parameters of the H-shaped steel object and its authentic specifications. This variance mainly emerges from the inclusion of connecting plates at the ends of certain STL models. Consequently, the measured length surpasses the length of the connecting plate. Furthermore, the length in the genuine specifications is solely calculated for standard H-section steel types, contributing to minor inconsistencies in length. While this matter has been acknowledged, it hasn't been rectified through program modification. This decision is influenced by the fact that the program doesn't generate errors while capturing the cross-sectional dimensions of the H-shaped steel object, and the accurate model can still be established. The second predicament pertains to the challenge of precisely retrieving the length and height dimension parameters for special type 7 H-shaped steel. This issue arises primarily due to the presence of both a partition and a connecting plate within the H-shaped steel structure, which confounds the algorithm's ability to accurately distinguish between these components.

ACKNOWLEDGMENTS

The authors extend their gratitude for the partially support provided for this research by the Taiwan Ministry of Science and Technology (MOST) / National Science and Technology Council (NSTC) under the grant numbers MOST-108-2221-E-008 -002 -MY3, MOST-109-2622-E-008 -018 -CC2, MOST- 110-2622-E-008 -018 -CC2, MOST-110-2221-E-008 -052 -MY3, NSTC-111-2622-E-008-017, and NSTC-111-2221-E-008 -027 -MY3. It is important to note that any opinions, findings, conclusions, and recommendations presented in this paper solely belong to the authors and do not necessarily reflect the perspectives of the MOST/NSTC.

REFERENCES

[1] Lyon, S.B., R. Bingham, and D.J. Mills (2017). "Advances in corrosion protection by organic coatings: What we know and what we would like to know." *Progress in Organic Coatings*, 102, 2-7.

[2] Bonner, P.E. and J.F. Stanners (2013). "Protection of steel by metal spraying: A review." *British Corrosion Journal*, 1(9), 339-343.

[3] Jamali, S. and D. Mills (2012). "Inhomogeneity of organic coatings and its effect of protection." *Annual Conference of the Australasian Corrosion Association*, 831-841.

[4] Huang, X., et al. (2016). "Automatic feature extraction and optimal path planning for robotic drawing." *IEEE International Conference on Cyber Technology in Automation, Control, and Intelligent Systems (CYBER)*, 19-24.

[5] Malu, G.M., S. Elizabeth, and S.M. Koshy (2018). "Circular mesh-based shape and margin descriptor for object detection." *Pattern Recognition*, 84, 97-111.

[6] Clément, M., C. Kurtz, and L. Wendling (2018). "Learning spatial relations and shapes for structural object description and scene recognition." *Pattern Recognition*, 84, 197-210.

[7] Huzurbazar, S., D. Kuang, and L. Lee (2019). "Landmark-based algorithms for group average and pattern recognition." *Pattern Recognition*, 86, 172-187.

[8] Armingol, J.M., et al. (2003). "Statistical pattern modeling in vision-based quality control systems." *Journal of Intelligent and Robotic Systems*, 37(3), 321-336.

[9] Balsamo, L., R. Betti, and H. Beigi (2014). "A structural health monitoring strategy using cepstral features." *Journal of Sound and Vibration*, 333(19), 4526-4542.

[10] Babi, M. (2019). "A Novel Method For Statistical Pattern Recognition Using The Network Theory And A New Hybrid System Of Machine Learning." *Materiali in Tehnologije*, 53(1), 95-100.

[11] Michaelsen, E. and J. Meidow (2014). "Stochastic reasoning for structural pattern recognition: An example from image-based UAV navigation." *Pattern Recognition*, 47(8), 2732-2744.

[12] Li, Q.X., et al. (2020). "Intelligent and automatic laser frequency locking system using pattern recognition technology." *Optics and Lasers in Engineering*, 126, 105881.

[13] Wallhäußer, E., et al. (2011). "On the usage of acoustic properties combined with an artificial neural network–A new approach of determining presence of dairy fouling." *Journal of Food Engineering*, 103(4), 449-456.

[14] Balsamo, L. and R. Betti (2015). "Data-based structural health monitoring using small training data sets." *Structural Control and Health Monitoring*, 22(10), 1240-1264.

[15] Kumar, A., et al. (2016). "A big data MapReduce framework for fault diagnosis in cloud-based manufacturing." *International Journal of Production Research*, 54(23), 7060-7073.

[16] Geisler, T. and A. Kolb (2018). "Pattern recognition of rough surfaces by using goniometric scattered light." *Metrology and Measurement Systems*, 25(1), 33-46.

[17] Kempf, R. and J. Adamy (2004). "Sequential pattern recognition employing recurrent fuzzy systems." *Fuzzy Sets and Systems*, 146(3), 451-472.

[18] Soualhi, M., K.T. Nguyen, and K. Medjaher (2020). "Pattern recognition method of fault diagnostics based on a new health indicator for smart manufacturing." *Mechanical Systems and Signal Processing*, 142, 106680.

[19] Nandhakumar, N. and J.K. Aggarwal (1985). "The artificial intelligence approach to pattern recognition—a perspective and an overview." *Pattern Recognition*, 18(6), 383-389.

[20] Vento, M. (2015). "A long trip in the charming world of graphs for pattern recognition." *Pattern Recognition*, 48(2), 291-301.

[21] Pichardo-Muñiz, A. (2011). "The role of diseconomies of transportation and public safety problems in the measurement of urban quality of life." *Applied Research in Quality of Life*, 6(4), 363-386.

[22] Chen, P.H. and L.M. Chang (2003). "Artificial intelligence application to bridge painting assessment." *Automation in Construction*, 12(4), 431-445.

[23] Wang, M. (2020). "Applying Internet information technology combined with deep learning to tourism collaborative recommendation system." *PLOS ONE*, 15(12), e0240656.

[24] Pathirage, C.S.N., et al. (2018). "Structural damage identification based on autoencoder neural networks and deep learning." *Engineering Structures*, 172, 13-28.

[25] Gasparetto, A., et al. (2012). "Automatic path and trajectory planning for robotic spray painting." *Proc., 7th German Conference on Robotics, ROBOTIK*, 1-6.

[26] Bai, Y. (2007). "Intelligent painting process planner for robotic bridge painting." *Journal of Construction Engineering and Management*, 133(4), 335-342.

[27] Qiao, L., A. Esmaeily, and H.G. Melhem (2012). "Signal pattern recognition for damage diagnosis in structures."

Computer‐Aided Civil and Infrastructure Engineering, 27(9), 699-710.

[28] Lu, W., et al. (2018). "Stress prediction for distributed structural health monitoring using existing measurements and pattern recognition." *Sensors*, 18(2), 419.

[29] Ma, X., et al. (2018). "Automatic detection of steel rebar in bridge decks from ground penetrating radar data." *Journal of Applied Geophysics*, 158, 93-102.

[30] Jingzhong, H., et al. (2018). "Strip Steel Surface Defects Recognition Based on SOCP Optimized Multiple Kernel RVM." *Mathematical Problems in Engineering*, 2018.

[31] Zeghal, M. and A.M. Abdel-Ghaffar (1992). "Analysis of behavior of earth dam using strong-motion earthquake records." *Journal of Geotechnical Engineering*, 118(2), 266-277.

[32] AbdelRazig, Y.A. and L.M. Chang (2000). "Intelligent model for constructed facilities surface assessment." *Journal of Construction Engineering and Management*, 126(6), 422-432.

[33] Zhang, M., W. Cheng, and Y. Wang (2018). "Multiple-fault classification for hot-mix asphalt production by machine learning." *Journal of Construction Engineering and Management*, 144(5), 04018024.

[34] Brilakis, I., S. German, and Z. Zhu (2011). "Visual pattern recognition models for remote sensing of civil infrastructure." *Journal of Computing in Civil Engineering*, 25(5), 388-393.

[35] Su, M.-C., et al. (2021). "Smart care using a DNN-based approach for activities of daily living (ADL) recognition." *Applied Sciences*, 11(1), 10.

APPENDIX A: Identification rates for six parameters for standard H-shaped modelled steel components

No.	Name	Length: correct recognition rate	Height: correct recognition rate	Width: correct recognition rate	Web thickness: correct recognition rate	Flange thickness: correct recognition rate
1	H 100x50x5x7x8	100%	100%	100%	100%	100%
2	H 100x100x6x8x8	100%	100%	100%	100%	100%
3	H 125x125x6.5x9x8	100%	100%	100%	100%	100%
4	H 150x75x5x7x8	100%	100%	100%	100%	100%
5	H 148x100x6x9x8	100%	100%	100%	100%	100%
6	H 150x150x7x10x8	100%	100%	100%	100%	100%
7	H 175x90x5x8x8	100%	100%	100%	100%	100%
8	H 175x175x7.5x11x13	100%	100%	100%	100%	100%
9	H 198x99x4.5x7x8	100%	100%	100%	100%	100%
10	H 200x100x5.5x8x8	100%	100%	100%	100%	100%
11	H 194x150x6x9x8	100%	100%	100%	100%	100%
12	H 200x200x8x12x13	100%	100%	100%	100%	100%
13	H 200x204x12x12x13	100%	100%	100%	100%	100%
14	H 248x124x5x8x8	100%	100%	100%	100%	100%
15	H 250x125x6x9x8	100%	100%	100%	100%	100%
16	H 244x175x7x11x13	100%	100%	100%	100%	100%
17	H 250x250x9x14x13	100%	100%	100%	100%	100%
18	H 250x255x14x14x13	100%	100%	100%	100%	100%
19	H 298x149x5.5x8x13	100%	100%	100%	100%	100%
20	H 300x150x6.5x9x13	100%	100%	100%	100%	100%
21	H 294x200x8x12x13	100%	100%	100%	100%	100%
22	H 298x201x9x14x13	100%	100%	100%	100%	100%
23	H 294x302x12x12x13	100%	100%	100%	100%	100%
24	H 300x300x10x15x13	100%	100%	100%	100%	100%
25	H 300x305x15x15x13	100%	100%	100%	100%	100%
26	H 304x301x11x17x13	100%	100%	100%	100%	100%
27	H 312x303x13x21x13	100%	100%	100%	100%	100%

No.	Name	Length: correct recognition rate	Height: correct recognition rate	Width: correct recognition rate	Web thickness: correct recognition rate	Flange thickness: correct recognition rate
28	H 318x307x17x24x13	100%	100%	100%	100%	100%
29	H 326x310x20x28x13	100%	100%	100%	100%	100%
30	H 346x174x6x9x13	100%	100%	100%	100%	100%
31	H 350x175x7x11x13	100%	100%	100%	100%	100%
32	H 336x249x8x12x13	100%	100%	100%	100%	100%
33	H 340x250x9x14x13	100%	100%	100%	100%	100%
34	H 350x252x11x19x13	100%	100%	100%	100%	100%
35	H 356x256x15x22x13	100%	100%	100%	100%	100%
36	H 364x258x17x26x13	100%	100%	100%	100%	100%
37	H 338x351x13x13x13	100%	100%	100%	100%	100%
38	H 344x348x10x16x13	100%	100%	100%	100%	100%
39	H 344x354x16x16x13	100%	100%	100%	100%	100%
40	H 350x350x12x19x13	100%	100%	100%	100%	100%
41	H 350x357x19x19x13	100%	100%	100%	100%	100%
42	H 360x354x16x24x13	100%	100%	100%	100%	100%
43	H 368x356x18x28x13	100%	100%	100%	100%	100%
44	H 378x358x20x33x13	100%	100%	100%	100%	100%
45	H 396x199x7x11x13	100%	100%	100%	100%	100%
46	H 400x200x8x13x13	100%	100%	100%	100%	100%
47	H 386x299x9x14x13	100%	100%	100%	100%	100%
48	H 390x300x10x16x13	100%	100%	100%	100%	100%
49	H 400x304x14x21x13	100%	100%	100%	100%	100%
50	H 410x308x18x26x13	100%	100%	100%	100%	100%
51	H 418x310x20x30x13	100%	100%	100%	100%	100%
52	H 388x402x15x15x22	100%	100%	100%	100%	100%
53	H 394x398x11x18x22	100%	100%	100%	100%	100%
54	H 394x405x18x18x22	100%	100%	100%	100%	100%
55	H 400x400x13x21x22	100%	100%	100%	100%	100%
56	H 400x408x21x21x22	100%	100%	100%	100%	100%

No.	Name	Length: correct recognition rate	Height: correct recognition rate	Width: correct recognition rate	Web thickness: correct recognition rate	Flange thickness: correct recognition rate
57	H 414x405x18x28x22	100%	100%	100%	100%	100%
58	H 428x407x20x35x22	100%	100%	100%	100%	100%
59	H 458x417x30x50x22	100%	100%	100%	100%	100%
60	H 446x199x8x12x13	100%	100%	100%	100%	100%
61	H 450x200x9x14x13	100%	100%	100%	100%	100%
62	H 456x201x10x17x13	100%	100%	100%	100%	100%
63	H 466x205x14x22x13	100%	100%	100%	100%	100%
64	H 478x208x17x28x13	100%	100%	100%	100%	100%
65	H 434x299x10x15x13	100%	100%	100%	100%	100%
66	H 440x300x11x18x13	100%	100%	100%	100%	100%
67	H 446x302x13x21x13	100%	100%	100%	100%	100%
68	H 450x304x15x23x13	100%	100%	100%	100%	100%
69	H 458x306x17x27x13	100%	100%	100%	100%	100%
70	H 468x308x19x32x13	100%	100%	100%	100%	100%
71	H 496x199x9x14x13	100%	100%	100%	100%	100%
72	H 500x200x10x16x13	100%	100%	100%	100%	100%
73	H 506x201x11x19x13	100%	100%	100%	100%	100%
74	H 512x202x12x22x13	100%	100%	100%	100%	100%
75	H 518x205x15x25x13	100%	100%	100%	100%	100%
76	H 528x208x18x30x13	100%	100%	100%	100%	100%
77	H 536x210x20x34x13	100%	100%	100%	100%	100%
78	H 548x215x25x40x13	100%	100%	100%	100%	100%
79	H 482x300x11x15x13	100%	100%	100%	100%	100%
80	H 488x300x11x18x13	100%	100%	100%	100%	100%
81	H 494x302x13x21x13	100%	100%	100%	100%	100%
82	H 500x304x15x24x13	100%	100%	100%	100%	100%
83	H 510x306x17x29x13	100%	100%	100%	100%	100%
84	H 518x310x21x33x13	100%	100%	100%	100%	100%
85	H 532x314x25x40x13	100%	100%	100%	100%	100%

No.	Name	Length: correct recognition rate	Height: correct recognition rate	Width: correct recognition rate	Web thickness: correct recognition rate	Flange thickness: correct recognition rate
86	H 596x199x10x15x13	100%	100%	100%	100%	100%
87	H 600x200x11x17x13	100%	100%	100%	100%	100%
88	H 606x201x12x20x13	100%	100%	100%	100%	100%
89	H 612x202x13x23x13	100%	100%	100%	100%	100%
90	H 618x205x16x26x13	100%	100%	100%	100%	100%
91	H 626x207x18x30x13	100%	100%	100%	100%	100%
92	H 634x209x20x34x13	100%	100%	100%	100%	100%
93	H 646x214x25x40x13	100%	100%	100%	100%	100%
94	H 582x300x12x17x13	100%	100%	100%	100%	100%
95	H 588x300x12x20x13	100%	100%	100%	100%	100%
96	H 594x302x14x23x13	100%	100%	100%	100%	100%
97	H 600x304x16x26x13	100%	100%	100%	100%	100%
98	H 608x306x18x30x13	100%	100%	100%	100%	100%
99	H 616x308x20x34x13	100%	100%	100%	100%	100%
100	H 628x312x24x40x13	100%	100%	100%	100%	100%
101	H 692x300x13x20x18	100%	100%	100%	100%	100%
102	H 700x300x13x24x18	100%	100%	100%	100%	100%
103	H 708x302x15x28x18	100%	100%	100%	100%	100%
104	H 712x306x19x30x18	100%	100%	100%	100%	100%
105	H 718x308x21x33x18	100%	100%	100%	100%	100%
106	H 732x311x24x40x18	100%	100%	100%	100%	100%
107	H 792x300x14x22x18	100%	100%	100%	100%	100%
108	H 800x300x14x26x18	100%	100%	100%	100%	100%
109	H 808x302x16x30x18	100%	100%	100%	100%	100%
110	H 816x306x20x34x18	100%	100%	100%	100%	100%
111	H 828x308x22x40x18	100%	100%	100%	100%	100%
112	H 890x299x15x23x18	100%	100%	100%	100%	100%
113	H 900x300x16x28x18	100%	100%	100%	100%	100%
114	H 912x302x18x34x18	100%	100%	100%	100%	100%

No.	Name	Length: correct recognition rate	Height: correct recognition rate	Width: correct recognition rate	Web thickness: correct recognition rate	Flange thickness: correct recognition rate
115	H 918x303x19x37x18	100%	100%	100%	100%	100%
Average Recognition Rate		**100%**	**100%**	**100%**	**100%**	**100%**

Note: the length, height, width, web thickness, and flange thickness of each data is written in order within the data name. (For example h 918x303x19x37x18 means that it has a length of 918mm, height of 303mm, width of 19mm, web thickness of 37mm, and flange thickness of 18mm).

APPENDIX B: Special Type of H-shaped steel

No.	Name	Size (mm)					Special Case
		Length	Height (H)	Width (B)	Web thickness (t1)	Flange plate thickness (t2)	
1	RH300X150X6.5X9X2878	2878	300	150	6.5	9	2
2	RH300X150X6.5X9X2878	2878	300	150	6.5	9	3
3	RH300X150X6.5X9X3213	3213	300	150	6.5	9	3
4	RH300X150X6.5X9X3213	3213	300	150	6.5	9	3
5	RH400X200X8X13X2296.5	2296.5	400	200	8	13	3
6	RH400X200X8X13X5588	5588	400	200	8	13	2
7	RH400X200X8X13X3094	3094	400	200	8	13	2
8	RH400X200X8X13X3213	3213	400	200	8	13	2
9	RH400X200X8X13X5598	5598	400	200	8	13	2
10	RH400X200X8X13X2883	2883	400	200	8	13	2
11	RH400X200X8X13X2193	2193	400	200	8	13	3
12	RH400X200X8X13X4588	4588	400	200	8	13	2
13	RH200X200X8X12X3330.6	3330.6	200	200	8	12	1
14	RH200X200X8X12X3116	3116	200	200	8	12	1
15	RH200X200X8X12X3782	3782	200	200	8	12	1
16	RH200X200X8X12X3928.5	3928.5	200	200	8	12	1
17	RH200X200X8X12X2279.2	2279.2	200	200	8	12	1
18	RH200X200X8X12X2445.8	2445.8	200	200	8	12	1
19	RH200X200X8X12X2288	2288	200	200	8	12	1
20	RH200X200X8X12X2215.7	2215.7	200	200	8	12	1
21	RH200X200X8X12X2375.1	2375.1	200	200	8	12	1
22	RH200X200X8X12X3219	3219	200	200	8	12	1
23	RH200X200X8X12X3005.3	3005.3	200	200	8	12	1

No.	Name	Size (mm)					Special Case
		Length	Height (H)	Width (B)	Web thickness (t1)	Flange plate thickness (t2)	
24	RH200X200X8X12X2218.1	2218.1	200	200	8	12	1
25	RH200X200X8X12X2867.2	2867.2	200	200	8	12	1
26	RH200X200X8X12X2714.5	2714.5	200	200	8	12	1
27	RH200X200X8X12X3431.1	3431.1	200	200	8	12	1
28	RH200X200X8X12X3197	3197	200	200	8	12	7
29	RH200X200X8X12X2018.1	2018.1	200	200	8	12	1
30	RH200X200X8X12X3458.7	3458.7	200	200	8	12	1
31	RH200X200X8X12X3923.5	3923.5	200	200	8	12	1
32	RH200X200X8X12X2358.1	2358.1	200	200	8	12	1
33	RH200X200X8X12X1599	1599	200	200	8	12	1
34	RH200X200X8X12X5064.5	5064.5	200	200	8	12	1
35	RH200X200X8X12X2086	2086	200	200	8	12	1
36	RH200X200X8X12X4336.8	4336.8	200	200	8	12	1
37	RH350X175X7X11X4688	4688	350	175	7	11	2
38	RH350X175X7X11X4688	4688	350	175	7	11	3
39	RH350X175X7X11X5784	5784	350	175	7	11	2
40	RH350X175X7X11X1684	1684	350	175	7	11	3
41	RH350X175X7X11X5688	5688	350	175	7	11	2
42	RH350X175X7X11X5688	5688	350	175	7	11	3
43	RH350X175X7X11X5688	5688	350	175	7	11	3
44	RH350X175X7X11X5688	5688	350	175	7	11	2
45	RH350X175X7X11X3813	3813	350	175	7	11	3
46	RH400X200X8X13X5688	5688	400	200	8	13	3
47	RH300X150X6.5X9X3813	3813	300	150	6.5	9	3

No.	Name	Size (mm)					Special Case
		Length	Height (H)	Width (B)	Web thickness (t1)	Flange plate thickness (t2)	
48	RH300X150X6.5X9X3813	3813	300	150	6.5	9	3
49	RH300X150X6.5X9X5688	5688	300	150	6.5	9	3
50	RH300X150X6.5X9X5688	5688	300	150	6.5	9	3
51	RH300X150X6.5X9X5784	5784	300	150	6.5	9	3
52	RH350X175X7X11X4688	4688	350	175	7	11	3
53	RH350X175X7X11X3813	3813	350	175	7	11	2
54	RH350X175X7X11X3813	3813	350	175	7	11	2
55	RH350X175X7X11X5688	5688	350	175	7	11	3
56	RH350X175X7X11X5688	5688	350	175	7	11	3
57	RH350X175X7X11X5688	5688	350	175	7	11	3
58	RH350X175X7X11X5688	5688	350	175	7	11	3
59	RH350X175X7X11X5688	5688	350	175	7	11	3
60	RH300X150X6.5X9X5743	5743	300	150	6.5	9	3
61	RH200X200X8X12X3062.5	3062.5	200	200	8	12	1
62	RH200X200X8X12X3347.5	3347.5	200	200	8	12	1
63	RH200X200X8X12X3062.5	3062.5	200	200	8	12	1
64	RH200X200X8X12X3440	3440	200	200	8	12	1
65	RH200X200X8X12X2995	2995	200	200	8	12	1
66	RH400X200X8X13X5820	5820	400	200	8	13	1
67	RH400X200X8X13X5774	5774	400	200	8	13	2
68	RH400X200X8X13X5860	5860	400	200	8	13	1
69	RH350X175X7X11X3855	3855	350	175	7	11	1
70	RH350X175X7X11X5780	5780	350	175	7	11	1
71	RH350X175X7X11X5820	5820	350	175	7	11	1

No.	Name	Size (mm)					Special Case
		Length	Height (H)	Width (B)	Web thickness (t1)	Flange plate thickness (t2)	
72	RH350X175X7X11X5774	5774	350	175	7	11	3
73	RH350X175X7X11X5860	5860	350	175	7	11	1
74	RH350X175X7X11X5860	5860	350	175	7	11	3
75	RH390X300X10X16X5820	5820	390	300	10	16	1
76	RH390X300X10X16X5820	5820	390	300	10	16	5
77	RH390X300X10X16X5860	5860	390	300	10	16	5
78	RH390X300X10X16X5860	5860	390	300	10	16	5
79	RH390X300X10X16X5780	5780	390	300	10	16	5
80	RH390X300X10X16X5780	5780	390	300	10	16	5
81	RH300X150X6.5X9X5734	5734	300	150	6.5	9	2
82	RH300X150X6.5X9X5780	5780	300	150	6.5	9	1
83	RH300X150X6.5X9X5780	5780	300	150	6.5	9	1
84	RH300X150X6.5X9X5780	5780	300	150	6.5	9	1
85	RH300X150X6.5X9X5734	5734	300	150	6.5	9	2
86	RH300X150X6.5X9X5734	5734	300	150	6.5	9	3
87	RH300X150X6.5X9X2878	2878	300	150	6.5	9	6
88	RH300X150X6.5X9X2878	2878	300	150	6.5	9	6
89	RH300X150X6.5X9X2878	2878	300	150	6.5	9	6
90	RH300X150X6.5X9X2883	2883	300	150	6.5	9	6
91	RH150X150X7X10X3205	3205	150	150	7	10	1
92	RH150X150X7X10X3805	3805	150	150	7	10	1
93	RH150X150X7X10X3086	3086	150	150	7	10	1
94	RH300X150X6.5X9X5598	5598	300	150	6.5	9	2
95	RH300X150X6.5X9X5598	5598	300	150	6.5	9	4

No.	Name	Size (mm)					Special Case
		Length	Height (H)	Width (B)	Web thickness (t1)	Flange plate thickness (t2)	
96	RH300X150X6.5X9X5598	5598	300	150	6.5	9	4
97	RH300X150X6.5X9X5688	5688	300	150	6.5	9	2
98	RH300X150X6.5X9X5688	5688	300	150	6.5	9	4
99	RH300X150X6.5X9X5688	5688	300	150	6.5	9	4